THE IMPACT OF ORBITAL AND CLOCK ERRORS ON POSITIONING FROM LEO CONSTELLATIONS AND PROPOSED ORBITAL SOLUTIONS

A. El-Mowafy[1*], K. Wang[2], Y. Li[3], A. Allahvirdi-Zadeh[4]

[1] School of Earth and Planetary Sciences, Curtin University, Australia, a.el-mowafy@curtin.edu.au
[2] National Time Service Center, Chinese Academy of Sciences, Xi'an; and University of Chinese Academy of Sciences, Beijing, China, wangkan@ntsc.ac.cn
[3] School of Surveying Engineering, East China University of Technology, China; and School of Earth and Planetary Sciences, Curtin University, Australia, yan.li@curtin.edu.au
[4] School of Earth and Planetary Sciences, Curtin University, Australia, amir.allahvirdizadeh@curtin.edu.au

KEY WORDS: LEO constellations, post-mission orbits, real-time orbits, clock stability, positioning and navigation

ABSTRACT:

Two approaches are discussed for the estimation and prediction of the orbits of low earth orbit (LEO) satellites that can be used for navigation. The first approach relays on using a ground monitoring network of stations. The procedures to generate the LEO orbital products in this approach are proposed at two accuracy levels to facilitate different positioning applications. The first type targets producing orbits at meter-level accuracy, defined here as LEO-specific broadcast ephemeris. The second type of products would produce orbits with an accuracy of cm as polynomial corrections to the first type of orbits. Real and simulated LEO satellite data is used for testing, mimicking LEO satellites that can be used for positioning. For the first type of products, it was found that orbital prediction errors play the dominant role in the total error budget, especially in cases of mid and long-term prediction. For the second type of products, the predicted orbits within a short period of up to 60 s generate errors at a few cm, and fitting the corrections with a quadratic polynomial reduced the fitting range errors to the cm level compared to the case of applying a linear polynomial. This level of accuracy can fulfill the requirement for precise point position[1]ing (PPP). The second approach is computing the orbits in real time applying the kinematic or reduced-dynamic mode, where the orbits are computed in the PPP mode using GNSS observations collected onboard LEO satellites and the GNSS orbits and clock products are received through inter-satellite links such as the free-access SouthPAN service in Australia, Galileo HAS, or Beidou (BDS-3, PPP-B2b service). The limitations of this approach and preliminary results are given. Furthermore, the LEO satellite clocks determined together with the orbits in the reduced-dynamic LEO satellite orbit process in near-real-time are also analysed. Finally, the impact of possible orbital and clock errors in the range of decimetres to several meters of LEO satellites on positioning performance is analysed.

1. INTRODUCTION

Precise positioning, navigation and timing (PNT) heavily rely on the use of Global Navigation Satellite Systems (GNSS), which are key to many essential applications in transport, defence, mining, construction, automation, space, agriculture, and national security. However, a known GNSS shortcoming is their weak signal strength, resulting in signal blockage by structures, and vulnerability to "spoofing" and radio frequency interference. Such shortcomings can be addressed to some extent through aiding GNSS by Low Earth Orbit (LEO) satellites, either by employing GNSS-like signals from dedicated LEO positioning systems or by the use of "signals of opportunity" from LEO mega-constellations that broadcast communication or internet signals, such as Starlink, Orbcomm and Iridium (Khalife, 202). These LEO satellites are approximately 20 times closer to Earth compared to the GNSS medium-earth orbit (MEO) satellites, with 300-1500km altitudes, and 90-120 minutes orbital periods. Hence, LEO satellites provide a new navigation space infrastructure of 300 to 2400 times more powerful signals than GNSS. This makes LEO signals more resilient to interference and available in deep attenuation settings, enabling positioning in challenging environments that have limited GNSS observations, such as in urban canyons, bushland, and rugged terrain.

Moreover, the corresponding high speed of LEO satellites enables faster satellite geometry change, thereby significantly shortening the convergence time for precise point positioning (PPP) (Wang et al., 2022). However, positioning from satellite signals requires knowledge of their orbits and clock behaviour, which are recently discussed in the literature (Allahvirdi-Zadeh et al., 2021, 2022a-c; Hauschild et al., 2022; Wang and El-Mowafy 2020, 2021; Wen et al., 2019). However, it is still a significant challenge for LEO. Firstly, the orbits of multiple LEO satellites need to be estimated and continually broadcast to users which require a dedicated infrastructure that need to be established. In addition, unlike GNSS satellites, and to reduce cost, weight, and power consumption, LEO satellites are not equipped with atomic clocks, and typically use oven-controlled crystal oscillators (OCXOs) or Ultra-Stable Oscillators (USOs), nor are they tightly time-synchronised with each other. These will impact the expected LEO-based positioning performance.

The paper briefly addresses the above points, which is organised as follows. The first two sections discuss the computation of the satellite orbits from a ground network presenting two approaches that give different accuracy levels, and a third approach for real-time onboard precise orbit determination using inter-satellite links. Next, LEO satellite clock performance is discussed with the

---

* Corresponding author

near-real-time clock precision and systematic effects analysed. Finally, the impact of the orbital and clock errors on the positioning performance is evaluated. The paper concludes with the main outcomes of this study.

2. COMPUTATION OF THE SATELLITE ORBITS FROM GROUND NETWORKS

The LEO orbital products computed by a ground network can be generated at two different levels of accuracy (Kan and El-Mowafy, 2020). Level-A products as a broadcast ephemeris type, computed in the post-processing mode at a master processing centre (MPC). The orbits are estimated by combining proper dynamic models with the GNSS observations collected onboard the LEO satellites, which are transmitted to ground monitoring stations (GMS) when LEO pass in the observation window of the GMS. The level-A products have an orbital accuracy at meter level, which is sufficient for applications such as single point positioning (SPP) or differential positioning, e.g. using the Real-Time Kinematic (RTK) method. The second type of products is a high-accuracy Level-B, at the dm level with a high sampling rate, which are corrections to broadcast ephemeris of Level-A orbits. Level-B is assumed to be transmitted via the Internet or satellite links, which can be used for PPP, benefiting from the rapid-varying LEO satellite geometry to reduce the solution convergence time and speed-up ambiguity solution.

Compared to the GNSS satellites, LEO satellites experience more complicated dynamics due to their lower altitudes, and as a result, suffer from higher influences of the Earth's gravitational field and air drag (Xie et al., 2018). Therefore, in this paper, 20 ephemeris parameters (given in Table 1), updated every 10 min, are used to fit the predicted orbits within a fitting interval of 20 min. The 20 ephemeris parameters include 16 parameters, similar to those of the GPS LNAV message with definitions given in (Wang and El-Mowafy, 2020), and four additional parameters that comprise the rate of the semi-major axis $\dot{a}$, the mean motion rate $\dot{n}$, and the amplitude of the two third-order harmonic (sine and cosine) correction terms to the orbit radius C_{rs3} and C_{rc3}.

Table 1. Ephemeris parameters expressing LEO satellite orbits

Category	Ephemeris parameters
GPS LNAV ephemeris parameters	$t_{oe}, \sqrt{a_0}, \Delta n, \Omega_0, I_0, \dot{I}, \dot{\Omega}, C_{us},$ $C_{uc}, C_{rs}, C_{rc}, C_{is}, C_{ic}$
Transformed GPS LNAV ephemeris parameters	e_x, e_y, λ_0
Additional ephemeris parameters	$\dot{a}, \dot{n}, C_{rs3}, C_{rc3}$

2.1 Level A products

The proposed Level A orbital products can be produced in the following steps (Kan and El-Mowafy, 2020). First, the GNSS data collected onboard the LEO satellites are downlinked to the GMSs and transferred to the MPC. The orbits are initialised by in-orbit SPP using the onboard GNSS code observations, which are initialized by using the two-line-elements (TLEs) orbits of the LEO satellites that have accuracy of several kilometers and are published and updated daily by the North American Aerospace Defense Command (NORAD). Next, high-accuracy reduced-dynamic orbits are processed with comprehensive dynamic

models, which are given in Table 2. The estimable dynamic parameters include the stochastic velocity pulses $\delta\boldsymbol{v}$ at pre-defined time points or piece-wise constant accelerations $\delta\boldsymbol{a}$ for pre-defined time intervals. The orbits are then predicted for several hours into the future with numerical integration. Subsequently, LEO-specific ephemeris parameters are estimated using the least-squares adjustment to describe the predicted orbits within a pre-defined fitting interval, which is much shorter than the prediction interval. The fitted ephemeris parameters are updated with an interval, so that overlapping time exists between two subsequent sets of the ephemeris parameters. All the estimated ephemeris parameters are then uplinked to the LEO satellites, and the LEO satellites broadcast their ephemeris parameters to users.

Table 2. Possible dynamic models used in processing of LEO orbits

Parameters	models
Earth gravity terms	EGM2008 (120degrees) (Pavlis, et al. 2008)
Gravity terms of other planets	JPL DE405 (Standish, 2020)
Solid Earth tides, Pole tides	IERS 2010 (Petit and Luzum, 2010)
Ocean tides	FES2004 (Lyard et al., 2006)

2.2 Level B products

Level-B products are assumed to be processed on the ground using high-accuracy real-time GNSS orbits and clocks and are predicted only for a short period compared to Level-A products (Wang and El-Mowafy, 2020). Level-B products are fitted into a low-order polynomial as corrections to the broadcast ephemeris, and are expressed as:

$$\boldsymbol{r}_B - \boldsymbol{r}_A = \boldsymbol{p}_0 + \boldsymbol{p}_1(t_i - t_0) + \cdots + \boldsymbol{p}_m(t_i - t_0)^m, \qquad (1)$$

where $\boldsymbol{r}_A$ and $\boldsymbol{r}_B$ represent the Level-A broadcast orbits and the short-term predicted precise orbits, respectively. $\boldsymbol{p}_k$ $(k = 0, \cdots, m)$ are the 3D polynomial coefficients with m denoting the highest polynomial degree. t_0 and t_i represent the correction reference time and the fitting time, respectively. In this study, 60 s interval is applied for the orbit prediction and using 1- to 3-degree polynomial fitting. The polynomial parameters and the matching reference time are then transmitted to users with a relatively high sampling rate, e.g. 10 s, via Internet or satellite links.

The possible performance of the two orbit-product levels is tested using the GRACE FO-1, as a representative example of LEO satellites, which has a low orbital height of about 500 km. For validation of the orbital errors, the precise orbits of GRACE FO-1 provided by the JPL are used as the reference [Wen et al., 2019)]. The real-time precise GPS orbits and clocks are obtained from the National Centre for Space Studies (CNES - France) (Laurichesse et al., 2013). The orbital errors are analyzed in terms of the 3D root-mean-square error (RMSE) and the orbital user range error (OURE), expressed as:

$$\text{OURE} = \sqrt{w_R^2\sigma_R^2 + w_{SW}^2(\sigma_S^2 + \sigma_W^2)}, \qquad (2)$$

where σ_R, σ_S and σ_W denote the RMS of the orbital errors in the radial, along-track and cross-track directions, respectively. The coefficients w_R and w_{SW} are related to the orbital height (Chen et

al., 2013), and assumed as 0.457 and 0.629 for GRACE FO-1 during the test period. The OURE and 3D RMSE error budget for the Level-A Product estimated at prediction periods of 0.5 hr to 2 hrs are given in table 3, and for the Level-B product using 1- to 3-degree polynomials are given in Table 4.

Table 3. Error budget of the Level-A products at prediction periods from 0.5 hr to 2 hrs

Prediction interval	OURE [m]			3D RMSE [m]		
	Prediction	Fitting	Total	Prediction	Fitting	Total
0.5 h	0.086	0.059	0.101	0.138	0.111	0.173
1 h	0.102	0.058	0.118	0.165	0.112	0.200
2 h	0.228	0.059	0.236	0.365	0.113	0.383

Table 4. Error budget of the Level-B orbital products with 60 s prediction time

Fitting type	Prediction errors [cm]		Fitting errors [cm]		Total errors [cm]	
	OURE	3D RMSE	OURE	3D RMSE	OURE	3D RMSE
Linear polynomial			0.5	0.9	2.59	4.56
Quadratic polynomial	2.5	4.4	0.1	0.2	2.53	4.44
Cubic polynomial			0.1	0.2	2.54	4.45

3. ONBOARD PRECISE ORBIT DETERMINATION

Kinematic Precise orbit determination (POD) and reduced-dynamic POD can also be applied in real-time onboard LEO satellites (Allahvirdi-Zadeh et al., 2022a). Onboard kinematic POD relies on precise positioning techniques applied in a filter that receives onboard GNSS observations, satellite attitude information from the attitude control system, and GNSS orbit and clock corrections from external sources. On the other hand, onboard reduced-dynamic POD involves propagating the orbit using basic dynamic models and refining it by integrating precise coordinates from kinematic POD. However, applying onboard POD is still challenging due to the various limitations. One limitation is the availability of orbit and clock corrections in space. This limitation is solved by recent advancements in the space links by GNSS and geostationary satellites that provide satellite-related corrections. For instance, Galileo provides High Accuracy Service (HAS) broadcasting orbit and clock corrections for GPS and Galileo constellations. By applying these corrections to GPS + Galileo observations, the orbital accuracy of the Sentinel-6A satellite has seen a 40% improvement compared to using only broadcast ephemeris (Hauschild et al., 2022). Regional services like Australian SouthPAN and Japanese MADOCA also made these free-of-charge corrections available in the Asia-Pacific region. For example, with these corrections applied in the POD, the GRACE-FO C and Sentinel-3B orbit validations have shown orbit accuracy within a few cm to decimeters based on the type of POD and the applied corrections (Allahvirdi-Zadeh et al., 2021). Table 5 summarizes the results of these studies.

Table 5. Summary of POD accuracy using GNSS orbit and clock corrections through various space links. (Kin and RD indicate kinematic and reduced-dynamic POD, respectively)

Limitation	Satellite	Solution	POD	3D Orbital accuracy (cm)
Availability of GNSS corrections	Sentinel-6A	Galilelo HAS	RD	6.9
	GRACE-FO C	SouthPAN (testbed)	RD	4.6
			Kin	14.3
		MADOCA	RD	2.3
			Kin	5.2
	Sentinel-3B	SouthPAN (testbed)	RD	6.2
			Kin	16.7
		MADOCA	RD	3.7
			Kin	7.7

Another solution to improve orbital accuracy with high-noise data is implementing a weighting function based on the Signal-to-Noise ratio of the actual observations, which enhanced the orbital accuracy and reduced observation residuals (Allahvirdi-Zadeh et al., 2022b). Additionally, an array of antennas and multi-constrained attitude determination using GNSS with ambiguity resolution can be implemented to address the limitations of high-noise attitude sensors (Allahvirdi-Zadeh & El-Mowafy, 2022a). This solution to attitude determination is more effective than getting the attitude from current magnetometers and sun sensors and costs less than accurate star trackers.

The accuracy of the onboard POD can be further improved by implementing inter-satellite ranges. Relative POD is necessary for formation flying missions and constellations. For example, evaluation of relative POD implemented using precise inter-satellite ranges between CubeSats from the Spire Global Constellation (https://spire.com), as an example of LEO satellites, has shown that these ranges can improve orbital accuracy within several decimetres (Allahvirdi-Zadeh & El-Mowafy, 2022b). Figure 1 represents applying inter-satellite links in onboard POD while the corrections are received through space links.

The stability of the onboard oscillator is another limitation of small LEO satellites, particularly CubeSats. These instabilities are observed in the receiver clock estimation as an output of POD. Possible reasons are the existing outliers in the observations, imperfect thermal control system, ignoring empirical phase centre variations of the onboard antenna (Allahverdi-Zadeh, 2021), higher order of relativity correction, and finally, the quality of the onboard oscillators. Some remedies and their impacts on clock stability are discussed in (Allahvirdi-Zadeh et al., 2022c).

The absolute and relative kinematic POD concept has been extended to include an undifferenced and uncombined approach (UDUC POD) instead of relying solely on the commonly used ionospheric-free (IF) linear observations. The UDUC algorithm and integer ambiguity resolution achieved a consistency of 2.8-3.8 cm in 3D with the reference orbits for T-A and T-B LEO satellites. This represents an improvement in orbital accuracy of 16.3% and 10.6% compared to the IF-based POD, respectively. Furthermore, the relative POD of the two satellites derived from the proposed model demonstrated a consistency of 1.1-1.5 mm (Mi et al., 2023).
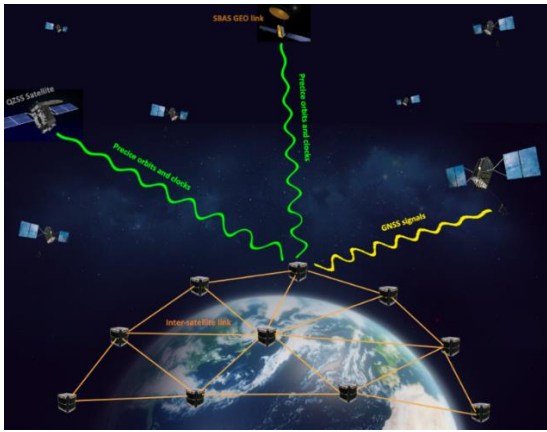
Figure 1. A demonstration of LEO constellations with inter-satellite links receiving GNSS orbit and clock corrections

4. ASSESSMENT OF LEO SATELLITE CLOCK PERFORMANCE

The LEO satellite clocks can be determined together with the orbits in the reduced-dynamic LEO satellite POD process in near-real-time.

4.1 Near-real-time clock precision

To assess the LEO satellite clock products, the CNES real-time service (RTS) GNSS clocks are re-referenced to the centre-of-mass (COM) final GNSS clocks by comparing the epoch-mean values between these two products for the GPS and the Galileo clocks, respectively. Taking the GPS+Galileo combined clock estimates using the COM final products as reference values, Figure 2 shows the clock errors of other solution types compared to the reference products for Sentinel-6A LEO satellite, considered as a representative example. A daily mean value is removed for each time series of the clocks to shift the mean to zero for a better comparison. From Fig. 2, it can be seen that clock errors generally lead to an STD at around 0.1 to 0.15 ns using the COM final products. The average STD from 1-7 February 2022 are listed in Table 6. The use of CNES RTS products slightly degraded the LEO satellite clock precision to about 0.15 to 0.2 ns. The differences between the GPS-only, Galileo-only and GPS+Galileo combined results are not significant.
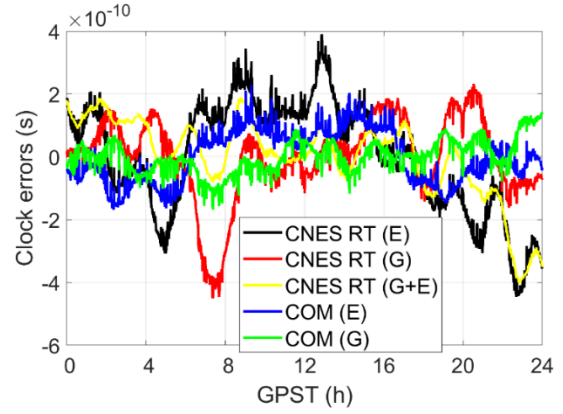
Figure 2. Clock errors of different solution types for Sentinel-6A on February 5, 2022. A daily mean value was removed for each clock time series.

Table 6. Averaged daily STD of the LEO satellite clock errors for Sentinel-6A using different GNSS measurements

GNSS Products	GPS+Galileo combined (ns)	GPS-only (ns)	Galileo-only (ns)
COM final	Reference	0.14	0.12
CNES RTS	0.16	0.16	0.18

4.2 Systematic effects

In this section, the Sentinel-6A clock behaviour is assessed over seven days (February 1-7, 2022), with the GPS+Galileo combined clocks estimated using the COM final products. As the COM GNSS satellite clocks are referenced to a different ground-based hydrogen maser from one day to another, to unify the time reference in this study, all the estimated LEO satellite clocks are re-referenced to the clock of the Galileo satellite E36 in the COM products, which used a passive hydrogen maser (PHM) and exhibited good stability over the entire test period, i.e., an averaged daily standard deviation of 6.0×10^{-11} s after detrending the data with a linear polynomial.

The left panel of Fig. 3 shows the 7-day clock behaviour of Sentinel-6A. The shifts at day boundaries were merged, and the plotted values were detrended with a best-fit linear polynomial. Note that a fourth-order polynomial clock was pre-corrected on a daily basis in the observation files provided by CSPDH (2023) to retag the observations to the GPS time scale (GPST).

From the left panel of Fig. 3, it can be observed that a half-day periodic effect with an amplitude of more than 2.5 m dominates all the systematic effects. This can also be confirmed through the Fast Fourier Transformation (FFT) spectrum of the data shown in the right panel of Fig. 3. Large systematic effects with similar periods were also observed in the GRACE Follow-on and Sentinel-3B satellites (Wang and El-Mowafy 2021), with the reason not yet totally identified. Compared to this large systematic effect, other secondary systematic effects also exist, including those with a period of 24 h, 8 h, 6 h, the once-per-revolution (1/rev) and the twice-per-revolution (2/rev) effects. The last two are related to the relativistic effects of the LEO satellites, possibly also influenced by other factors, for instance, voltage variation (Larson et al. 2007). They become insignificant compared to other systematic effects for LEO satellites at this height, i.e., more than 1300 km.

Figure 4. The skyplot of 240 LEO at 1000 km and GPS over a 20 minutes period in Curtin University's CUT000 site
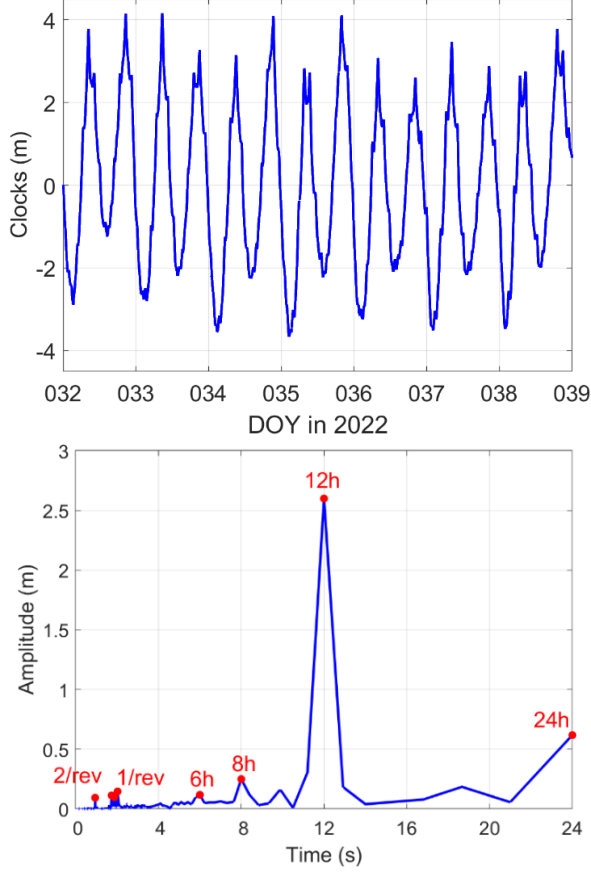
Figure 3. (Left) Detrended and re-referenced LEO satellite clock estimates in meters and (right) its FFT spectrum using the Sentinel-6A data

The mid- to long-term systematic effects were shown to vary from satellite to satellite, and even in time. Before the reasons for these effects are totally understood, mid- to long-term prediction of such clocks becomes difficult as only mathematical models derived from empirical analysis can be used. Based on the results shown in Wang and El-Mowafy (2021), a 10 min prediction leads already to RMSE of more than 1 dm even with different systematic effects considered in the prediction model. In such cases, the prediction is limited to short-term for real-time applications requiring high-accuracy LEO satellite clocks.

5. IMPACT OF ORBITAL AND CLOCK ERRORS ON POSITIONING

Having briefly discussed the LEO orbital estimation methods and limitations and clock error behaviour, this section demonstrates their impact on positioning results. To this end, one needs first to discuss which constellation is assessed. Our research and others (e.g. Li et al., 2019) have shown that a constellation of 192 or 240 near-polar-orbit LEO-supported navigation satellites at an altitude of about 1000 km would allow observing about 6-7 satellites simultaneously from most regions on Earth, which would enable positioning and navigation. For example, Figure 4 shows the sky distribution of 240 LEO constellation and GPS over a duration of 20 minutes above Curtin University's CUT000 site in Western Australia. Although both LEO and GPS constellations exhibit similar GDOP values, the LEO satellites demonstrate significantly faster orbital motion and satellite elevation changes compared to the GPS satellites.
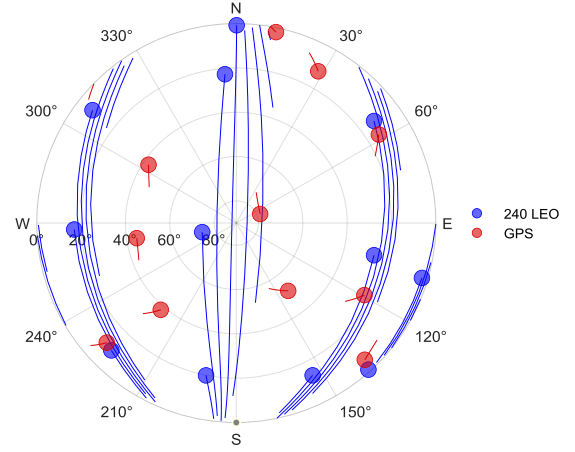
The projection of the orbital and clock errors on the signal direction eventually influences the positioning of the users (Wang et al., 2022). The orbital user range errors (OURE) and clock user range errors (CURE) can be used to evaluate the preliminary impact of the orbital and clock errors on positioning, which can be expressed as:

$$IMP_{orb} = GDOP \cdot \sigma_{OURE} \tag{3}$$

$$IMP_{cl} = GDOP \cdot \sigma_{CURE} = GDOP \cdot (\sigma_\tau \cdot \tau \cdot c) \tag{4}$$

where IMP_{orb} represents the impact of satellite orbital error, σ_{OURE} represents the orbital user range error, IMP_{cl} represents the impact of satellite clock error, σ_{CURE} represents the clock user range error, σ_τ is the Allan variance which represents the clock stability, τ represents the period of the clock predictions, c represents the speed of light. GDOP denotes the geometry dilution of precision which maps the number and geometry of observed satellites onto the expected positioning error.

Given the values of GDOP, possible orbital and clock errors, the orbital error influence IMP_{orb} and clock error influence IMP_{cl} are computed based on equations (3) and (4). The maximum GDOP values for this constellation within a 24-hour period for different regions on earth with clear sky visibility range from 0.9 to 3.6. The prediction OUREs of three LEO satellites (GRACE C satellite, Sentinel-1A and Sentinel-3B) exhibit difference in the range of cm to several meters, due to orbital altitudes, the selected prediction strategy, fitting interval and the prediction period (Wang et al., 2022). The frequency stability of the oscillator is responsible for the clock error, and the Allan variance is commonly used to express the frequency instability. Larger LEO satellites such as GRACE and COSMIC-2 are typically equipped with highly precise oscillators that offer stabilities in the range of 10^{-14} to 10^{-12}. However, it has been observed that COSMIC satellites exhibit clock stabilities at the level of 10^{-11} to 10^{-9}. Additionally, clock stability tests have revealed variations in the range of 10^{-11} to 10^{-9} among different CubeSats over a period of 1 second (Allahvirdi-Zadeh et al., 2022). Therefore, this study primarily analyze the impact of cm to meter level satellite OUREs (0.05m, 0.1m, 0.5m, 1m, 5m, 10m) and satellite clock stabilities ranging from 10-13~10-8 with $\tau = 1s$.

Figure 5 shows the impact of different OUREs and satellite clock errors on the positioning utilising simulated observations from the 240 LEO satellites at 1000 km constellation. The upper and lower

critical values of GDOP are 0.9 in the polar regions and 3.6 near the equator. Therefore, in polar regions, the impacts of OUREs are nearly equal to the orbital user range errors, while in the vicinity of the equator, the impacts is three times that of OUREs. In Figure 5(a), the impact on positioning error is 9 m in polar regions and 36 m in equatorial regions when the OURE is 10 m. The impact on positioning error is 0.045 m in polar regions and 0.18 m in equatorial regions when the OURE is 0.05 m. In Figure 5(b), When the stability of satellite clocks is at 10^{-8}, the impact on positioning error is approximately 3 meters in polar regions and 11 meters in equatorial regions. When the stability of satellite clocks is at 10^{-10}, the impact on positioning error is 0.027 meters in polar regions and 0.108 meters in equatorial regions. When the stability of satellite clocks exceeds 10^{-11}, the impact of satellite clock errors on global positioning error is less than 0.011 meters. The specific values of the impact are summarised in Table 7.

6. CONCLUSIONS

Achieving reliable PNT from constellations relays on the availability of precise orbits and clock information to users. This is a challenging task as it requires infra structure, and as most LEO satellite do not operate with atomic clocks. In this study, three procedures to provide the LEO orbital products are discussed. The first is with a relatively low accuracy at sub-m, i.e., the Level A products, and the second is high-accuracy LEO orbital products at less than 10 cm, i.e., the Level B products. These orbits are proposed to be processed on the ground through a monitoring and processing facility. The GNSS collected onboard LEO are used with good dynamic models, extrapolated to up to several hours and tens of seconds for the Level A and B products, respectively. The third approach is based on real-time processing of the collected GNSS observations onboard LEO satellites, and broadcast these to users. Their accuracy can range from a few cm to 15 cm.

Clock errors with relatively reasonable stability lead to a STD at around 0.1 to 0.15 ns using rapid precise products, and the use of real-time products slightly degraded the LEO satellite clock precision to about 0.15 to 0.2 ns. The differences between using GPS-only, Galileo-only and GPS+Galileo combined observations onboard LEO did not lead to significant changes for clock estimation and prediction. The clocks are also impacted by significant systematic effects. These mid- to long-term systematic effects were shown to vary from satellite to satellite, and a 10 min prediction leads already to RMSE of more than 1 dm. The impact of the orbital errors and clock instability for a LEO constellation of 240 satellites with 1000 km altitude ranged similarly from the dm to m levels, depending of the values of the orbital and clock errors and the number and geometry of observed satellites.
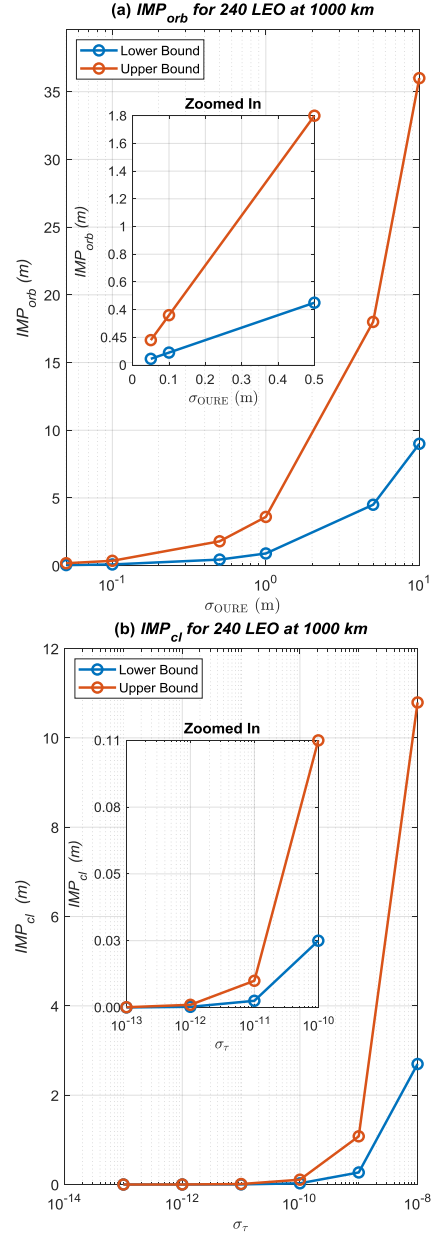
Figure 5. The impact of satellite orbital user range errors (0.05m, 0.1m, 0.5m, 1m, 5m, 10m) and clock stabilities ($10^{-13} \sim 10^{-8}$) on global positioning with 240 LEO at 1000 km (The lower and upper values with the maximum GDOP used are 0.9 to 3.6)

Table 7. Impact of satellite orbital user range errors (OUREs) and clock stabilities on global positioning with 240 LEO at 1000 km

	OUREs (m)	**0.05**	**0.1**	**0.5**	**1**	**5**	**10**
IMP_{orb} (m)	Upper values (GDOP=3.6 near the equator)	0.18	0.36	1.8	3.6	18	36
	Lower values (GDOP=0.9 in polar regions)	0.045	0.09	0.45	0.9	4.5	9
	Clock stabilities ($\tau = 1s$)	**10^{-13}**	**10^{-12}**	**10^{-11}**	**10^{-10}**	**10^{-9}**	**10^{-8}**
IMP_{cl} (m)	Upper values (GDOP=3.6 near the equator)	1×10^{-4}	1×10^{-3}	0.011	0.108	1.08	10.8
	Lower values (GDOP=0.9 in polar regions)	3×10^{-5}	3×10^{-4}	3×10^{-3}	0.027	0.27	2.7

REFERENCES

Allahvirdizadeh, A. 201). Phase centre variation of the GNSS antenna onboard the CubeSats and its impact on precise orbit determination. In *GSA Earth Sciences Students Symposium-WA (GESSS-WA)*. doi.org/10.13140/RG.2.2.10355.45607/1

Allahvirdi-Zadeh, A., Wang, K., & El-Mowafy, A. 2021. POD of small LEO satellites based on precise real-time MADOCA and SBAS-aided PPP corrections. *GPS solutions*, *25*(31), 1-14. doi.org/10.1007/s10291-020-01078-8

Allahvirdi-Zadeh, A., Wang, K., & El-Mowafy, A. 2022a. Precise Orbit Determination of LEO Satellites Based on Undifferenced GNSS Observations. *Journal of surveying engineering*, *148*(1), 03121001. doi.org/10.1061/(ASCE)SU.1943-5428.0000382

Allahvirdi-Zadeh, A., El-Mowafy, A., & Wang, K. 2022b. *Precise Orbit Determination of CubeSats Using Proposed Observations Weighting Model*. In (pp. 1-8). Springer Berlin Heidelberg. doi.org/10.1007/1345_2022_160

Allahvirdi-Zadeh, A., Awange, J., El-Mowafy, A., Ding, T., & Wang, K. 2022c. Stability of CubeSat Clocks and Their Impacts on GNSS Radio Occultation. *Remote Sensing*, *14*(2), 1-26. doi.org/10.3390/rs14020362

Allahvirdi-Zadeh, A., & El-Mowafy, A. 2022a. CubeSat's attitude determination using GNSS antenna array. *International Global Navigation Satellite Systems Conference (IGNSS) 2022*, UNSW, Sydney. doi.org/10.13140/RG.2.2.29925.68320

Allahvirdi-Zadeh, A., & El-Mowafy, A. 2022b. The impact of precise inter-satellite ranges on relative precise orbit determination in a smart CubeSats constellation. *EGU General Assembly Conference*, Vienna, Austria. doi.org/10.5194/egusphere-egu22-2215

Chen, L.; Jiao, W.; Huang, X.; Geng, C.; Ai, L.; Lu, L.; Hu, Z. 2013. Study on signal-in-space errors calculation method and statistical characterization of BeiDou navigation satellite system. In Proceedings of the China Satellite Navigation Conference (CSNC) 2013; Sun, J., Jiao, W., Wu, H., Shi, C., Eds.; *Lecture Notes in Electrical Engineering,* Volume 243; Springer: Berlin, Heidelberg, Germany, 2013

Hauschild, A., Montenbruck, O., Steigenberger, P., Martini, I., & Fernandez-Hernandez, I. 2022. Orbit determination of Sentinel-6A using the Galileo high accuracy service test signal. *GPS solutions*, *26*(4), 120. https://doi.org/10.1007/s10291-022-01312-5

Khalife, J.; Neinavaie, M.; Kassas, Z.M. 2020. Navigation with differential carrier phase measurements from Megaconstellation LEO satellites. *In Proceedings of the 2020 IEEE/ION PLANS*, Portland OR, USA, 20-23 April 2020.

Larson KM, Ashby N, Hackman C, Bertiger W. 2007. An assessment of relativistic effects for low Earth orbiters: the GRACE satellites. Metrologia, 44(6): 484-490. doi: 10.1088/0026-1394/44/6/007

Laurichesse, D.; Cerri, L.; Berthias, J.P.; Mercier, F. 2013. Real time precise GPS constellation and clocks estimation by means of a Kalman filter. *In Proceedings of the ION GNSS+ 2013*, Nashville, TN, USA, 16–20 September 2013; pp. 1155–1163.

Li, X., Ma, F, Li, X, Lv, H, Bian, L, Jiang, Z, Zhang, X. 2019. LEO constellation-augmented multi-GNSS for rapid PPP convergence*, Journal of Geodesy* 93:749–764.

Lyard, F.; Lefevre, F.; Letellier, T.; Francis, O. 2005. Modelling the global ocean tides: Modern insights from FES2004. *Ocean Dyn.* 2006, 56, 394–415.

Mi, X., Allahvirdi-Zadeh, A., El-Mowafy, A., Huang, Z., Wang, K., Zhang, B., & Yuan, Y. 2023. Absolute and relative POD of LEO satellites in formation flying: Undifferenced and uncombined approach. *Advances in Space Research*, 1-29. https://doi.org/10.1016/j.asr.2023.05.024

Pavlis, N.K.; Holmes, S.A.; Kenyon, S.C.; Factor, J.K. 2008. An Earth gravitational model to degree 2160: EGM2008. *EGU 2008*, Vienna, Austria, 13–18 April 2008.

Petit, G.; Luzum, B. 2010. IERS Conventions. *IERS Technical Note, 36*. Frankfurt am Main: Verlag des Bundesamts für Kartographie und Geodäsie, 2010. 179 pp., ISBN: 3-89888-989-6, 2010.

Standish, E.M. 1998. *JPL Planetary and Lunar Ephemerides*, DE405/LE405. JPL IOM 312, F-98-048, 1998.

Wang K, El-Mowafy A. 2021. LEO satellite clock analysis and prediction for positioning applications. *Geo-spatial Information Science*, 25(1):14-33. doi: 10.1080/10095020.2021.1917310

Wang. K., El-Mowafy A. 2020. Proposed orbital products for positioning using mega-constellation LEO satellites. *Sensors,* 2020, 20, 5806; doi:10.3390/s20205806

Wang, K., Allahvirdi-Zadeh, A., El-Mowafy, A., & Gross, J. N. 2020. A Sensitivity Study of POD Using Dual-Frequency GPS for CubeSats Data Limitation and Resources. *Remote Sensing*, *12(13):2107*. https://doi.org/10.3390/rs12132107

Wang, k., El-Mowafy, A., Wang, W., Yang, L., Yang X. 2022. Integrity Monitoring of PPP-RTK positioning with LEO. Part II:LEO augmentation. *Remote Sensing*. *14*(7), 1599; doi.org/10.3390/rs14071599.

Wen, H.Y.; Kruizinga, G.; Paik, M.; Landerer, F.; Bertiger, W.; Sakumura, C.; Bandikova, T.; Mccullough, C. 2019. *Gravity recovery and climate experiment follow-on (GRACE-FO) Level-1 data product user handbook*. JPL D-56935 (URS270772), NASA Jet Propulsion Laboratory, California Institute of Technology, September 11, 2019.

Xie, X.; Geng, T.; Zhao, Q.; Liu, X.; Zhang, Q.; Liu, J. 2018. Design and validation of broadcast ephemeris for low Earth orbit satellites. *GPS Solutions*. 2018, 22, 54.